Eur Biophys J (2011) 40:529–543
DOI 10.1007/s00249-011-0676-5

ORIGINAL PAPER

Irregular structure of the HIV fusion peptide in membranes demonstrated by solid-state NMR and MD simulations

Dorit Grasnick · Ulrich Sternberg · Erik Strandberg · Parvesh Wadhwani · Anne S. Ulrich

Received: 9 October 2010 / Revised: 21 December 2010 / Accepted: 11 January 2011 / Published online: 28 January 2011

Abstract To better understand peptide-induced membrane fusion at a molecular level, we set out to determine the structure of the fusogenic peptide FP23 from the HIV-1 protein gp41 when bound to a lipid bilayer. An established solid-state ^{19}F nuclear magnetic resonance (NMR) approach was used to collect local orientational constraints from a series of CF_3-phenylglycine-labeled peptide analogues in macroscopically aligned membranes. Fusion assays showed that these ^{19}F-labels did not significantly affect peptide function. The NMR spectra were characteristic of well-behaved samples, without any signs of heterogeneity or peptide aggregation at 1:300 in 1,2-dimyristoyl-*sn*-glycero-3-phosphatidylcholine (DMPC). We can conclude from these NMR data that FP23 has a well-defined (time-averaged) conformation and undergoes lateral diffusion in the bilayer plane, presumably as a monomer or small oligomer. Attempts to evaluate its conformation in terms of various secondary structures, however, showed that FP23 does not form any type of regular helix or β-strand. Therefore, all-atom molecular dynamics (MD) simulations were carried out using the orientational NMR constraints as pseudo-forces to drive the peptide into a stable alignment and structure. The resulting picture suggests that FP23 can adopt multiple β-turns and insert obliquely into the membrane. Such irregular conformation explains why the structure of the fusion peptide could not be reliably determined by any biophysical method so far.

Keywords HIV-1 protein gp41 · Membrane fusion · Fusogenic peptides · Solid-state ^{19}F- and ^{2}H-NMR · β-Stranded secondary structure · All-atom MD simulations

Introduction

The HIV-1 protein gp41 carries a fusogenic sequence that is responsible for triggering fusion of the viral membrane with the target cell (White et al. 2008). The N-terminal fragment of 23 residues is active even in isolation; hence, this so-called fusion peptide FP23 is regarded as a suitable model in biophysical investigations (Durell et al. 1997). Its three-dimensional structure has been extensively studied in membrane-mimicking environments to learn more about the mechanism of fusion. However, no clear picture has emerged so far, given that α-helical or β-stranded secondary structures, and sometimes a mixture of both, have been reported. Qualitative conformational analysis by circular dichroism (CD) revealed a helical structure of the fusion peptide in 40% TFE, 1% sodium dodecyl sulfate (SDS), or in 1-palmitoyl-2-oleoyl-*sn*-glycero-3-phosphatidylcholine (POPC)/1-palmitoyl-2-oleoyl-*sn*-glycero-3-phosphatidylglycerol (POPG) vesicles (Chang et al. 1997a, b; Sackett et al. 2009; Kliger et al. 1997; Li and Tamm 2007; Pritsker et al. 1998), while CD and Fourier-transform infrared (FTIR) measurements at high peptide concentration or in uncharged vesicles

Membrane-active peptides: 455th WE-Heraeus-Seminar and AMP 2010 Workshop.

Electronic supplementary material The online version of this article (doi:10.1007/s00249-011-0676-5) contains supplementary material, which is available to authorized users.

D. Grasnick · A. S. Ulrich (✉)
Karlsruhe Institute of Technology,
Institute of Organic Chemistry and CFN,
Fritz-Haber-Weg 6, 76131 Karlsruhe, Germany
e-mail: anne.ulrich@kit.edu

U. Sternberg · E. Strandberg · P. Wadhwani · A. S. Ulrich
Karlsruhe Institute of Technology, Institute of Biological Interfaces (IBG-2), POB 3640, 76021 Karlsruhe, Germany

suggested a β-stranded conformation (Haque et al. 2005; Pritsker et al. 1999; Gerber et al. 2004; Sackett and Shai 2003; Peisajovich et al. 2000; Rafalski et al. 1990; Pereira et al. 1997). Solid-state NMR was used to characterize the local backbone conformation of FP23 and its analogues in lipid bilayers, revealing α-helical or β-stranded structures depending on the sample conditions and lipid composition (Yang et al. 2001; Wasniewski et al. 2004; Bodner et al. 2008; Qiang et al. 2007, 2009; Sackett et al. 2010). Namely, in cholesterol-free membranes a helical conformation dominated, in the presence of negatively charged lipids both structures were present, whereas in a lipid mixture resembling that of the target membrane mainly oligomeric β-stranded conformations were found (Li and Tamm 2007; Yang et al. 2001; Yang and Weliky 2003; Wasniewski et al. 2004; Bodner et al. 2008; Qiang et al. 2008). Especially when trimerically linked peptide constructs were investigated, β-sheets dominated (Yang et al. 2003; Zheng et al. 2006; Qiang and Weliky 2009). Then again, high-resolution ^{1}H-NMR analysis of FP23 in detergent micelles showed a largely helical conformation (Jaroniec et al. 2005; Chang et al. 1999), compared with previous observations of a shorter helical stretch and additional β-elements (Chang et al. 1997a, b), or a β-sheet structure derived by combined MD and NMR analysis in dimethyl sulfoxide (DMSO) (Kanyalkar et al. 2004). An FTIR study of FP23 in lipid vesicles deduced a membrane-inserted β-stranded N-terminus with a C-terminal α-helix on the bilayer surface (Peisajovich et al. 2000), whereas MD simulations starting with a full-length α-helix suggested an overall insertion angle of about 40° in the membrane (Maddox and Longo 2002; Wong 2003).

The numerous studies under various different conditions demonstrate that FP23 is conformationally flexible and able to assume rather different structures depending on its environment (Gabrys and Weliky 2007; Li and Tamm 2007). However, a consistent trend emerges, namely that a conversion from a monomeric α-helix to β-stranded aggregates is triggered by increasing the peptide-to-lipid ratio (Rafalski et al. 1990), by inducing oligomerization (Gordon et al. 2002, 2004), or by compression of the peptide in the membrane (Barz et al. 2008; Castano and Desbat 2005). Similar structural plasticity has also been described for other fusogenic peptides, which often have the potential to form some kind of helix but tend to aggregate as oligomeric β-sheets (Afonin et al. 2004; Glaser et al. 1999; Gordon et al. 2008; Ulrich et al. 1999). It thus appears that folding and aggregation is a critical step that converts an active fusion peptide into an inactive end-product (Wadhwani et al. 2010). The challenge in searching for a meaningful structure is therefore to find appropriate sample conditions that are biologically relevant but where aggregation has not yet taken place. A lipid bilayer is clearly the most preferential environment, but peptide aggregation is strongly promoted in the membrane-bound state. That is because the molecules accumulate at the bilayer surface, where they are preordered and highly likely to encounter each other to oligomerize and aggregate, in a series of steps that may well resemble the actual fusion event. In a biological context, one may expect that the trimeric GP41 protein can expel three fusion peptides at the same time, but for symmetry reasons these are located on three opposite faces of the complex. In the very first step of fusion, when the fusion peptide leaves its protein pocket to meet the lipid bilayer, it is thus most likely monomeric. Oligomerization and/or aggregation of FP23 will then occur rapidly in the plane of the membrane when several such trimers come together to form the site of fusion.

The aim of the present study is to find NMR conditions where membrane-bound FP23 is still monomeric and at the same time well structured, i.e., representing the moment of membrane insertion. Solid-state ^{19}F-NMR is a highly sensitive method that provides local orientational parameters and readily allows peptide aggregation to be monitored in oriented samples (Wadhwani et al. 2008). NMR spectra of selectively ^{19}F-labeled peptide analogues are acquired to first monitor the overall sample homogeneity and molecular mobility, and then to calculate the alignment of the peptide backbone in the membrane from the dipolar NMR constraints. An analogous structure analysis has been previously carried out for another fusogenic peptide involved in fertilization (Afonin et al. 2004; Glaser et al. 1999). This highly sensitive ^{19}F-NMR approach has been extensively applied to a diverse range of well-folded peptides (1) to confirm their expected α-helical or β-stranded conformation in the membrane, (2) to determine their molecular alignment in the lipid bilayer (Afonin et al. 2003, 2004, 2008a, b; Glaser et al. 2005; Grage et al. 2010; Maisch et al. 2009; Mykhailiuk et al. 2006, 2008; Salgado et al. 2001; Strandberg et al. 2006, 2008; Strandberg and Ulrich 2004; Tremouilhac et al. 2006a, b; Ulrich 2005, 2007; Ulrich et al. 2006; Wadhwani et al. 2008), and more recently even (3) to examine the amplitudes of fluctuation for these stiff secondary structure elements in liquid-crystalline membranes (Esteban-Martín et al. 2009, 2010; Strandberg et al. 2009). In the present ^{19}F-NMR study of membrane-bound FP23, we have also collected several orientational constraints and examined these data as to whether they support any of the suggested well-defined secondary structures (α-helix, 3_{10}-helix, π-helix, extended or twisted β-strand). However, none of these regular conformations was found to be compatible with our NMR data. Therefore, we combined the orientational constraints with MD simulations (Sternberg et al. 2007) to search for an NMR-consistent conformation and alignment of FP23 in membranes. In a 10 ns MD run a stable backbone

conformation was identified, which turned out to be rather irregular with several β-turns.

Materials and methods

Peptide–lipid samples for NMR

To label FP23 (AVGIGALFLGFLGAAGSTMGARS-$CONH_2$) for ^{19}F-NMR, 4-CF_3-*L*-Phenylglycine (CF_3-Phg, from ABCR, Karlsruhe, Germany) was used to replace one by one the amino acids Leu7, Phe8, Leu9, Phe11, and Leu12, which are similarly bulky and hydrophobic. Four ^{2}H-labeled analogues were produced with a single 2,2,2-$^2H_3$-*L*-alanine (D_3-Ala, from Cambridge Isotope Laboratories, Andover, MA, USA) in place of Ala6, Leu7, Ala14 or Ala15. These ^{19}F- or ^{2}H-labeled peptides were synthesized by standard solid-phase Fmoc protocols, the *D*- and *L*-epimers of racemic CF_3-Phg were assigned, and the products were purified by high-performance liquid chromatography (HPLC) as described in the Electronic Supporting Material (ESM) and previous protocols (Afonin et al. 2003, 2004; Glaser et al. 2005; Salgado et al. 2001). The lipids 1,2-dimyristoyl-*sn*-glycero-3-phosphatidylcholine (DMPC), 1-palmitoyl-2-oleoyl-*sn*-glycero-3-phosphatidylcholine (POPC), and 1-palmitoyl-2-oleoyl-*sn*-glycero-3-phosphatidylglycerol (POPG) were obtained from Avanti Polar Lipids (Alabaster, AL, USA).

Macroscopically oriented NMR samples were prepared on glass plates by depositing a co-solubilized lipid–peptide mixture from chloroform/water/methanol, drying, and subsequent rehydration (see ESM) (Afonin et al. 2003, 2004; Glaser et al. 2005; Salgado et al. 2001). For ^{19}F-NMR, oriented samples were prepared with two different peptide-to-lipid molar ratios (P/L) of 1:30 or 1:300 in DMPC, and with 1:300 in a POPC/POPG 4/1 mixture. Additionally, nonoriented samples were prepared as multilamellar vesicle (MLV) dispersions containing the ^{19}F-labeled peptides at a 1:30 ratio in DMPC with excess water. For ^{2}H-NMR, macroscopically oriented samples were prepared with the ^{2}H-labeled peptides at P/L = 1:300 in DMPC.

Solid-state NMR experiments and data analysis

All solid-state ^{19}F- and ^{2}H-NMR measurements were carried out on a Bruker Avance 500 MHz spectrometer (Bruker Biospin, Karlsruhe, Germany) at 35°C, and ^{31}P-NMR spectra were recorded to check the quality of lipid alignment (see ESM for details of the experimental parameters). For ^{19}F- and ^{2}H-NMR measurements the sample was aligned first with its normal parallel to the static magnetic field direction, and in a second experiment it was aligned perpendicular. For the structure calculation all dipolar couplings in the parallel sample alignments are measured, and their signs are determined from the respective chemical shift, being positive for signals that occur downfield of the isotropic position (Afonin et al. 2008a, b; Glaser et al. 2005; Salgado et al. 2001; Ulrich 2005; Wadhwani et al. 2008).

To interpret the NMR data in terms of the peptide structure and alignment in the membrane, three types of order parameters have to be considered. (1) The bilayer order parameter S_b: For molecules that rotate fast in the bilayer plane, we get $S_b = 1.0$ when the sample normal is aligned parallel to B_0, and $S_b = -0.5$ for the perpendicular case (see previous paragraph). (2) The local order parameter of the measured molecular segment S^i_{loc}: This parameter may differ for individual labeled positions in regions of different mobility within a peptide. For dipolar interactions it can usually be approximated by an axially symmetric tensor. (3) The molecular order parameter S_{mol}: This Saupe parameter describes the overall alignment of the molecule in the bilayer, which generally requires a biaxial definition. In some rod-like systems the contribution of biaxiality can be neglected, but there is no general rule as to when it may be dropped. If the biaxiality is neglected, we obtain the following formula for the observed splitting (Marsan et al. 1999):

$$\Delta\nu_i = C\, S_b S^i_{loc} S_{mol} \frac{3\cos^2\theta_i - 1}{2}. \quad (1)$$

The dipolar splitting $\Delta\nu_i$ of an individual label i thus depends on the angle θ_i between the rotational axis of the rapidly spinning CF_3-group and the static magnetic field direction, as well as on the local order parameter S^i_{loc}. The constant C of the static dipolar ^{19}F-^{19}F coupling of a CF_3-group at room temperature must be known to calculate the peptide structure. Because of the strong $1/r^3$ dependence of the dipolar coupling, even vibrational effects on the F–F distance cannot be neglected. From the static molecular model of trifluorotoluene with C–F distances of 1.322 Å (mean value of 309 compounds) (Allen et al. 1987), we calculated a fundamental coupling of 16.6 kHz for a rotating CF_3-group. Since C–F bond and F–C–F angle vibrations will lead to even larger couplings, we decided to use the mean value of 16.975 kHz obtained from NMR investigations on CF_3-phenyl compounds (Dürr 2005).

In the case of a well-folded peptide with a regular structure (such as an α-helix) and with rigidly attached labels (such as the CF_3-Phg labels used here), Eq. (1) can be simplified, since $S^i_{loc} = 1$ for all positions. In this case θ_i can also be stated as a function of τ and ρ and some fixed parameters defining the regular structure of the peptide (Strandberg et al. 2004; Glaser et al. 2005). If an oriented sample is aligned in the field such that $S_b = 1$, the helix

orientation in the membrane can be readily calculated from a number of splittings measured for several labels as local orientational constraints. The overall molecular alignment is then described by three parameters, namely by the tilt angle τ of the dominant symmetry axis of the peptide with respect to the bilayer normal, by the azimuthal rotation angle ρ around this axis, and by the molecular order parameter S_{mol}. This kind of analysis has been performed for a wide range of different membrane-bound peptides (Afonin et al. 2008a, b; Glaser et al. 2005; Grage et al. 2010; Maisch et al. 2009; Mykhailiuk et al. 2008; Salgado et al. 2001; Strandberg and Ulrich 2004; Strandberg et al. 2006, 2008; Tremouilhac et al. 2006a, b; Ulrich 2005, 2007; Ulrich et al. 2006; Wadhwani et al. 2008). Assuming, for example, a helical conformation of the peptide, the tilt τ represents the angle between the helix axis (directed from N- to C-terminus) and the bilayer normal. The azimuthal angle ρ corresponds to a right-handed rotation around the helix axis, for which we define $\rho = 0^\circ$ as the orientation when the vector projecting radially through the C^α atom of Leu12 is aligned parallel to the membrane plane. For the data analysis we modeled the peptide FP23 as several different types of idealized regular structures, namely an α-helix, 3_{10}-helix, π-helix, and a β-strand, as described previously (Glaser et al. 2004, 2005; Maisch et al. 2009). Based on these parameters, the alignment of the peptide was fitted to the five orientational constraints from the ^{19}F-NMR experiments. The best-fit values of τ, ρ, and S_{mol}, which gave the smallest root-mean-square deviation (RMSD) between experimental and calculated couplings, were assessed by a grid search procedure (Strandberg et al. 2006; Tremouilhac et al. 2006b; Ulrich 2005). Obviously, such a fitting procedure and grid search breaks down when the actual conformation of the peptide does not correspond to any of the assumed structural models, or when the peptide possesses regions of significantly different mobility along its backbone.

Molecular dynamics simulation with orientational constraints

It has been previously demonstrated that MD simulations with orientational constraints (MDOC) allow the calculation of NMR splittings as time averages of the corresponding dipolar or quadrupolar tensors (Sternberg et al. 2007). These simulations are performed *in vacuo*, and the orienting influence of the anisotropic membrane environment is mimicked by orientational pseudo-forces derived from the NMR parameters. The pseudo-forces $\boldsymbol{F}$ are derivatives of pseudo-energies that are added to the force field energy:

$$F^{\mathrm{A}}_{x_{ij}} = k \sum_{\alpha\beta}^{3} \left(P^{theo_{\mathrm{A}}}_{\alpha\beta} - P^{\exp_{\mathrm{A}}}_{\alpha\beta} \right) \frac{\partial}{\partial x_{\gamma_j}} P^{theo_{\mathrm{A}}}_{\alpha\beta}$$
$$\frac{\partial}{\partial x_{\gamma_j}} P^{theo_{\mathrm{A}}}_{\alpha\beta} = \left(D_{\beta\beta'} \frac{\partial}{\partial x_{\gamma_j}} D_{\alpha\alpha'} + D_{\alpha\alpha'} \frac{\partial}{\partial x_{\gamma_j}} D_{\beta\beta'} \right) P^{theo_{\mathrm{A}}}_{\alpha'\beta'}. \quad (2)$$

The pseudo-forces contain Cartesian derivatives (denoted by the Greek index γ; the Einstein sum convention is used) of the transformation matrices $\boldsymbol{D}$ which connect the local molecular coordinate systems (denoted by "A") with the laboratory system. When applying the pseudo-forces power during the MD run, molecular rotations and reorientations are stimulated to satisfy these extra constraints. The pseudo-forces will become zero once the calculated splittings have reached the same values as the experimental ones.

From the orientation of these tensors [denoted by P in Eq. (2) and depicted in Fig. 7 as tensor ellipsoids with cut corners for the principal axes] at every MD time step an order parameter analysis can be performed that is independent of Eq. (1) (Sternberg et al. 2007). Such MD analysis can thus yield a structural description that is valid even when faced with an unexpected peptide conformation or dynamic profile. The molecular and local order parameters, S_{mol} and S^i_{loc}, can be extracted directly from the MD simulation, since the orientation of the interaction tensor and its time development can be incrementally sampled at every time step. The local order tensors S^i_{loc} are calculated from the mean values of the principal axes of the dipolar tensors within the laboratory system, and the molecular order tensor S_{mol} is obtained from the principal axes of inertia of the peptide, whichever conformation it assumes. From a principal axes transformation of these tensors the order parameters and biaxialities are obtained. Therefore the order parameters S_{mol} and S^i_{loc} determined from the MD simulation are not the same as those in Eq. (1), where biaxiality is neglected.

As a starting structure for the NMR-constrained MD simulation, we chose a partly helical model of FP23 that had been published on the basis of infrared (IR) and MD studies in hexafluoroisopropanol (Gordon et al. 2002, 2004). We extracted the first of 19 models from a protein data bank file, which is helical between Ala2 and Gly13 (Fig. 6). We added four water molecules to Arg22 and three water molecules to the N-terminus, because charged groups would form strong hydrogen bonds to the peptide backbone. The water molecules shield these groups and lead to more realistic structures in the presence of water. The simulation contains a total of 359 atoms, including the 7 water molecules. An advantage of our MDOC simulations is that oriented media such as membranes do not need to be included explicitly in the

simulation. Simulations that include all-atom membrane models are computationally still too slow to be able to cover molecular reorientations on the timescale observed in NMR experiments. Provided that sufficiently long all-atom MDOC simulations are performed, the starting conformation is of minor concern. During the MDOC run, in each of the five ^{19}F-labeled positions of FP23 the local orientational constraint measured from the corresponding CF_3-group was applied as a pseudo-force to align the C^{α}–C^{β} bond vector of the native amino acid. In this way the constraints can be implemented without the need to introduce any perturbing "mutations" in the peptide structure. From the two NMR measurements with the membrane normal parallel and perpendicular to the magnetic field we know the complete dipolar CF_3 tensors including the sign of the dipolar coupling. This information is important since every component of the calculated tensor can be assigned to a direction within the laboratory frame and the complete tensor can be used as an orientational constraint.

Two MDOC runs were performed using the simulation parameters as given in the ESM. After the first MDOC run of 1 ns, a long 10 ns run was performed to track possible changes of the molecular conformation. To obtain an *NTV* ensemble (with conserved particle number *N*, temperature *T*, and volume *V*), we introduced a proper thermostating procedure (Evans and Morris 1990). This procedure rescales the velocities and forces in such a way that the temperature fluctuates about a selected mean value. Thermostating was essential since prevailing differences between the constraints and their calculated values are sources of heat. In contrast to traditional MD simulations we had to introduce procedures to control the pseudo-forces (Sternberg et al. 2007). The first possibility to scale down the pseudo-forces can be derived from the fast rotation of the peptide around the membrane director. We therefore calculated rotational mean values of the dipolar coupling tensors with respect to the membrane normal. Nevertheless, at the start of the simulation no motional averaging had occurred yet, and the pseudo-energy amounted to 3528 kJ/mol. This is of the same order of magnitude as the total electrostatic energy. The pseudo-forces were therefore stepped up exponentially from zero with a time constant of 200 ps. The same time constant value was used for the memory time of the time average of the dipolar couplings, to ensure that the calculated dipolar couplings are mainly sampled from the end of the simulation. The pseudo-force width ensures that these forces do not rise linearly with the difference to the experiment but become nearly constant if this difference gets much larger than ΔP (see Table S2 in ESM).

Results

To collect orientational constraints for the membrane-bound HIV fusion peptide, a number of NMR labels have to be selectively incorporated into FP23. We decided to use the rigid CF_3-Phg for highly sensitive solid-state ^{19}F-NMR analysis, as well as D_3-Ala for nonperturbing ^{2}H-NMR observation (Glaser et al. 2005; Strandberg et al. 2006; Tremouilhac et al. 2006a, b). Since these reporter groups are rigidly attached to the peptide framework, each local orientation constraint reflects the alignment of the corresponding backbone segment. If the molecule assumes a well-defined secondary structure such as an α-helix or β-strand, it will be possible to calculate its overall alignment from the set of NMR parameters.

To select positions in FP23 that can be labeled without interfering with the peptide structure or function, we consulted previous mutational studies on both the isolated fusion peptide and the full-length protein gp41 (Buchschacher et al. 1995; Delahunty et al. 1996; Jaroniec et al. 2005; Mobley et al. 1999; Pritsker et al. 1998; Reichert et al. 2007; Sackett and Shai 2002; Wong 2003; Yang et al. 2003, 2004). CF_3-Phg was thus used to replace Leu7, Phe8, Leu9, Phe11 or Leu12, which have a similar bulk and hydrophobicity, while D_3-Ala was substituted for Ala6, Leu7, Ala14 or Ala15. Most other residues, such as glycine and valine, have been reported to be very sensitive to mutations; hence, we refrained from placing any labels there. In total, nine differently labeled FP23 analogues were prepared (see Table S1 in ESM). All CF_3-Phg-containing peptides have previously been examined by circular dichroism and showed very similar spectra with a high degree of α-helical structure in TFE (Reichert et al. 2007). Lipid mixing assays and dynamic light scattering were used to characterize the kinetics of peptide-induced fusion of large unilamellar vesicles. Again, incorporation of CF_3-*L*-Phg into FP23 did not have any significant impact on function (Reichert et al. 2007). Interestingly, the corresponding *D*-epimeric peptides, which had been obtained as side-products from the incorporation of racemic CF_3-Phg, did not show any systematic differences in their fusogenic activity either. Significant differences would have been expected for the case that FP23 were to assume a regular secondary structure in the rate-determining step of fusion, in view of the pronounced steric restrictions imposed by the rigid CF_3-*D*-Phg side-chain. From these kinetic observations it could therefore be concluded that FP23 does not require any well-defined conformation in the actual process of vesicle fusion (Reichert et al. 2007).

Orientational constraints were collected from the ^{19}F-labeled peptides by standard solid-state NMR experiments using macroscopically oriented membrane samples,

as described earlier (Afonin et al. 2008a, b; Glaser et al. 2005; Grage et al. 2010; Maisch et al. 2009; Mykhailiuk et al. 2008; Salgado et al. 2001; Strandberg and Ulrich 2004; Strandberg et al. 2006, 2008; Tremouilhac et al. 2006a, b; Ulrich 2005, 2007; Ulrich et al. 2006; Wadhwani et al. 2008). Two samples with different peptide-to-lipid ratios of P/L = 1:300 and 1:30 were investigated to cover a low-concentration and a high-concentration range. The quality of the aligned membranes was checked by ^{31}P-NMR, which showed well-oriented lamellar signals for 1:300 and a slight degree of misalignment at P/L = 1:30 (data not shown). The ^{19}F-NMR spectra of the five CF_3-Phg labeled peptides at P/L = 1:300 in DMPC are shown in Fig. 1. Each spectrum displays one well-resolved dipolar triplet due to the homonuclear dipolar coupling of the CF_3-group (Table 1). The observation of relatively narrow lines with different couplings clearly indicates that (1) the lipid–peptide samples are homogeneous under these conditions, and (2) that FP23 assumes a distinct structure in the membrane, at least as a time average on the millisecond timescale.

To examine the mobility of the peptide and check for signs of aggregation, each sample was measured in a parallel as well as perpendicular alignment between the

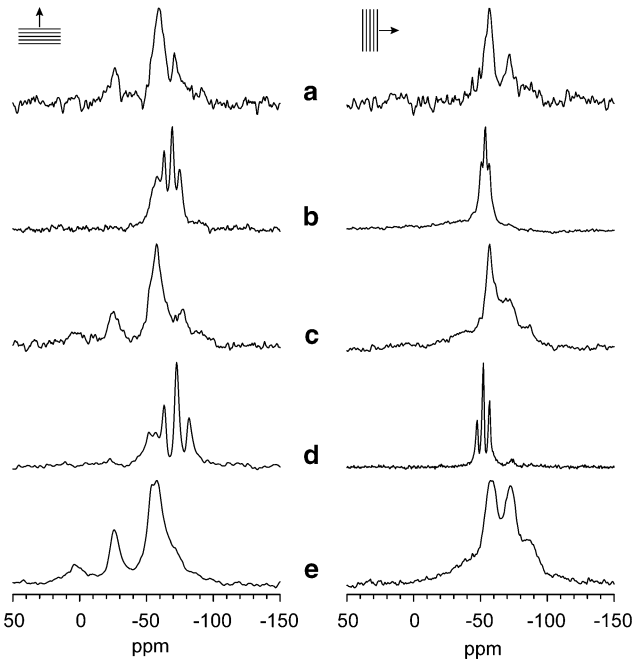

Fig. 1 ^{19}F-NMR spectra of the fusion peptide FP23 from the protein gp41 of HIV-1, labeled with CF_3-Phg in the position of Leu7 (**a**), Phe8 (**b**), Leu9 (**c**), Phe11 (**d**) or Leu12 (**e**), and reconstituted in DMPC at a peptide-to-lipid ratio of 1:300. The oriented NMR samples were measured at 35°C with the membrane normal parallel to the magnetic field (0° tilt) and in a perpendicular orientation (90° tilt). The signed dipolar couplings are used as orientational constraints in the structure analysis of FP23

Table 1 Dipolar couplings from experiment and MD simulation, for the individual CF_3-Phg-labeled segments on FP23, measured by ^{19}F-NMR in oriented DMPC at 1:300 (0° tilt), or produced accordingly by 10 ns MD

Labeled in position on FP23	Leu7	Phe8	Leu9	Phe11	Leu12
Experimental splitting (kHz)	14.2	−2.8	12.8	−4.4	15.8
Splitting from MD (kHz)	14.2	−2.2	9.5	−3.8	13.8

bilayer normal and the magnetic field. A well-resolved triplet with a distinct dipolar coupling should be obtained in the parallel aligned samples. In the perpendicular sample, this coupling will be scaled by a factor of −0.5 in cases where the peptide is motionally averaged about the membrane normal, whereas a powder-like line shape will be observed for immobile peptides (Afonin et al. 2008a, b; Glaser et al. 2005; Salgado et al. 2001; Ulrich 2005; Wadhwani et al. 2008). If, however, already the spectrum of the parallel sample alignment looks like a powder, this is a sign that the peptide does not have any preferred orientation and is thus inhomogeneously aggregated. Since the dipolar couplings for FP23 at P/L = 1:300 in DMPC changed by a factor of −0.5 when the bilayer normal was changed from a parallel to a perpendicular orientation relative to the external magnetic field (see Eq. 1 and Table S3 in ESM), we conclude that FP23 undergoes fast motional averaging about the membrane normal at P/L = 1:300. At such low peptide concentration we can conclude that the fusion peptide must be present in DMPC as a monomer or small oligomer, with a unique, possibly time-averaged conformation.

A different situation was encountered in oriented samples at a high P/L of 1:30. All FP23 analogues gave the same powder line shape with a coupling of 15.8 kHz (data not shown), corresponding to a spinning but otherwise static CF_3-group which lacks any preferred alignment in the sample. This observation indicates that the peptide is (1) no longer oriented homogeneously in the membrane, and (2) has become immobilized. We thus conclude that at high concentration FP23 tends to aggregate and loses its well-defined alignment in the lipid bilayer. Some nonoriented multilamellar dispersion samples with the ^{19}F-labeled FP23 analogues in DMPC confirmed the structural interpretation above (see ESM), but demonstrated that the cationic fusion peptide is only weakly attracted by zwitterionic DMPC and tends to partition into the bulk water phase. We therefore included negatively charged lipids in oriented POPC/POPG samples containing FP23 at P/L = 1:300. The corresponding dipolar couplings essentially confirmed the analysis in DMPC, but there were several signs to suggest that FP23 has a stronger tendency to aggregate in the presence of anionic lipids than in DMPC (see Table S3 in ESM).

Besides the five ^{19}F-labeled analogues of FP23, we also prepared four peptides with D_3-Ala, namely in positions Ala6, Leu7, Ala14, and Ala15. Since the quadrupolar couplings of these CD_3-groups can be analyzed analogously to the CF_3-groups (Afonin et al. 2003; Strandberg et al. 2006; Tremouilhac et al. 2006a, b; Ulrich 2005), we had intended to collect additional orientational constraints for comprehensive structural analysis of FP23. However, the ^{2}H-NMR spectra of these peptides at P/L = 1:300 in oriented DMPC bilayers did not reveal any signals from the peptides (see Fig. S1 in ESM), and only some natural abundance intensity from the lipids could be detected. Despite the lower sensitivity of ^{2}H- compared with ^{19}F-NMR, other peptides have been successfully analyzed by ^{2}H-NMR at comparably low concentration (Strandberg et al. 2006, 2008). Hence, it seems that in the case of FP23 dynamic effects on the microsecond timescale may have prevented picking up the quadrupolar splittings with an echo sequence (in contrast to the one-pulse ^{19}F experiments) at 35°C in liquid-crystalline DMPC.

RMSD analysis of peptide conformation and alignment

As we had successfully done with many other peptides before, we set out to analyze the secondary structure of FP23 and to calculate its molecular alignment in DMPC at P/L = 1:300. A detailed description of this procedure has been published in previous research papers and reviews (Afonin et al. 2003, 2008a, b; Glaser et al. 2005; Salgado et al. 2001; Ulrich 2005; Wadhwani et al. 2008). Briefly, the peptide is modeled with a regular secondary structure (see "Materials and methods"), whose alignment in the membrane coordinate system is described in terms of a tilt angle τ and an azimuthal rotation angle ρ. Any wobbling of the peptide backbone in the membrane is accounted for by a molecular order parameter S_{mol} (disregarding biaxiality effects). This factor scales down the dipolar couplings relative to the static values, and it can take values between $S_{mol} = 1$ (no wobble) and 0 (isotropic averaging). At this point of our FP23 analysis it is important to note that many of the dipolar couplings in Table 1 are very large and close to the maximum static coupling constant $C = 16.975$ kHz (Eq. 1). Under the initial assumption that FP23 may be regarded as a rigidly folded body, this observation would imply that it does not wobble in liquid-crystalline DMPC (i.e., $S_{mol} \approx 1$), despite the fact that it undergoes long-axial rotation about the membrane normal on the millisecond timescale (Glaser et al. 2005; Strandberg et al. 2008). Such behavior may either be attributed to our oversimplified analysis (see below), or to the formation of small oligomers which hold each other steady. The latter situation has been observed before for several other membrane-active peptides in an oligomeric transmembrane alignment, such as gramicidin S and alamethicin (Afonin et al. 2008a; Maisch et al. 2009).

As a starting point for the structural analysis of FP23, we generated four different models with regular secondary structures, namely α-helix, 3_{10}-helix, π-helix, and β-strand. The geometry of each model is defined by characteristic backbone torsion angles as reported (Glaser et al. 2004; Maisch et al. 2009). Each conformational model was subjected to a grid search by systematically varying the angular parameters τ and ρ, as well as S_{mol}. The calculated dipolar couplings were compared with the experimental data of all five ^{19}F-labeled positions, and the resulting root mean square deviation (RMSD) contour plots are shown in Fig. 2 for FP23 in DMPC at P/L = 1:300. The best-fit values are listed in Table S4 in the ESM for these DMPC samples and for the other ones mentioned. For any of the underlying conformational models examined, the best-fit combination of τ and ρ is considered to represent the most likely alignment of such putative peptide structure in the lipid bilayer. At first sight the lowest RMSD values are found to correspond to an α-helix or a 3_{10}-helix aligned at a tilt of $\tau \approx 90°$ relative to the membrane surface, i.e., with the helix lying flat in the bilayer plane (see Fig. 2a and c, and further discussion in ESM). However, even these RMSD values are much higher than in any of our previous studies of other membrane-bound peptides. Hence, none of the four conformational models (α-helix, 3_{10}-helix, π-helix, β-strand) yields a convincing picture of membrane-bound FP23. We conclude that the peptide does not seem to adopt a regular secondary structure with stable hydrogen bonds, which may not even be surprising in view of the many ambiguities and apparent contradictions in previous structural studies (Bodner et al. 2008; Castano and Desbat 2005; Chang et al. 1997a, b, 1999; Gabrys and Weliky 2007; Gerber et al. 2004; Gordon et al. 2002, 2004; Jaroniec et al. 2005; Kliger et al. 1997; Li and Tamm 2007; Maddox and Longo 2002; Peisajovich et al. 2000; Pritsker et al. 1998, 1999; Qiang et al. 2008; Rafalski et al. 1990; Reichert et al. 2007; Sackett and Shai 2003; Wasniewski et al. 2004; Wong 2003; Yang and Weliky 2003; Yang et al. 2001, 2003; Zheng et al. 2006).

An RMSD plot represents an overall fit to all five orientational constraints at the same time. In case there might be a single local perturbation in an otherwise regular structure, we examined whether any one data point might deviate significantly from the resulting best-fit structure. The dipolar wave plots of Fig. 2 display all experimental data points individually, to be compared with the expected values that are represented by a curve over 360° around the helical wheel of the corresponding regular secondary structure. Inspection of this wave plot for the α-helical model (Fig. 2b) does not reveal any single point that would explain the high RMSD. The CF_3-Phg label in position

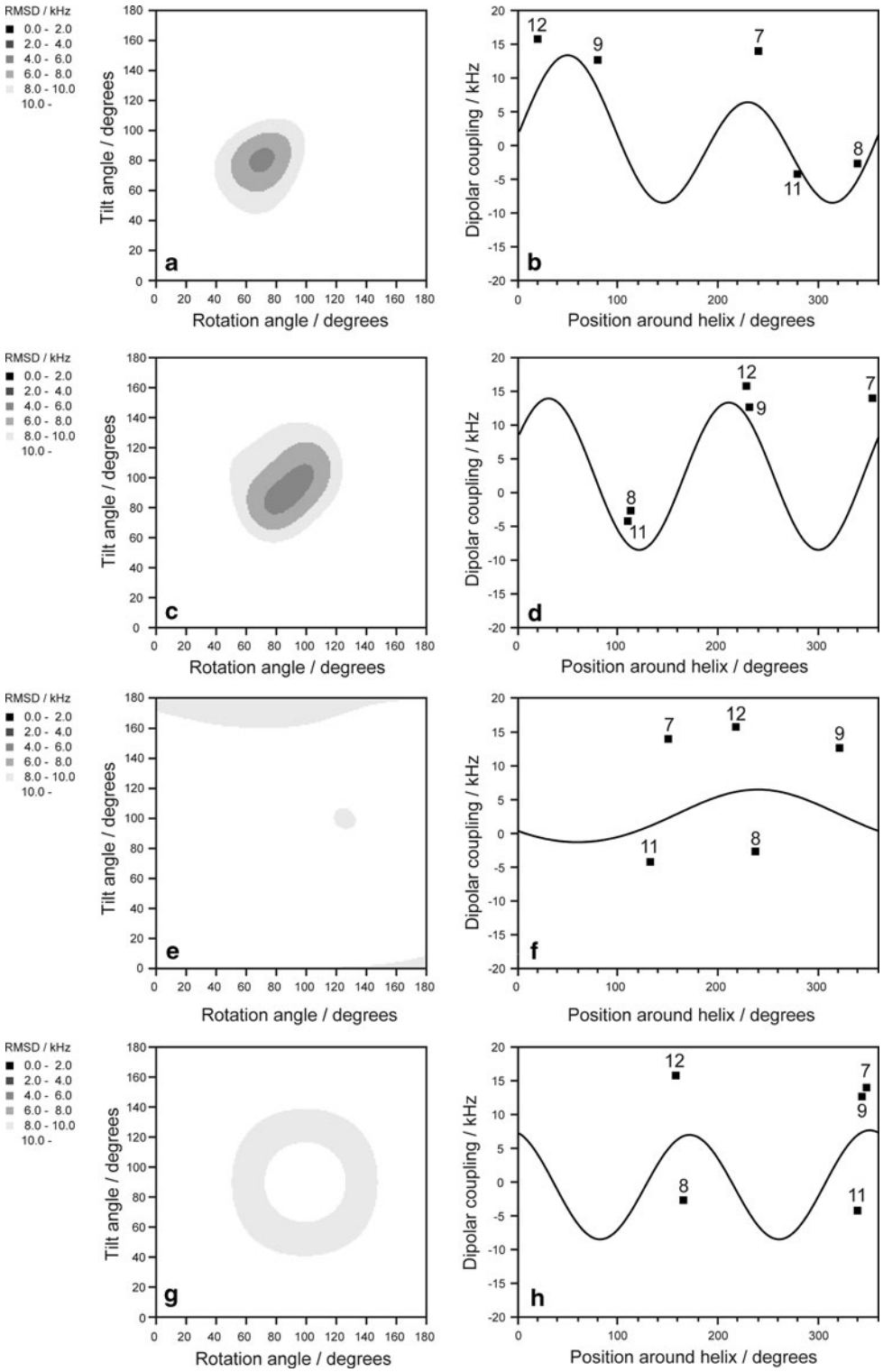

Fig. 2 RMSD analysis (*left* panels) and helical wave plots (*right* panels) from the ^{19}F-NMR dipolar couplings of FP23 in oriented DMPC at a peptide-to-lipid ratio of 1:300. **a**, **b** α-helix; **c**, **d** 3_{10}-helix; **e**, **f** π-helix; **g**, **h** β-sheet

Leu7 might be questioned, but RMSD analysis without this value does not give a significantly improved solution either. By excluding two points for Leu7 and Phe12 it is possible to get a better fit, but such a procedure cannot be justified. The possibility of a 3_{10}-helix gives a similarly poor fit as an α-helix, as both the RMSD and the plots in Fig. 2c and d do not differ much from the interpretation of FP23 as an α-helix (see also ESM). It is also obvious that

the π-helix (Fig. 2e, f) or β-strand (Fig. 2g, h) models give even worse fits with extremely high RMSD values. Even if a β-strand was slightly twisted as might be expected for an oligomeric β-sheet, such pattern would display only a gradual shift of couplings compared with the current analysis, which is not observed.

There are obviously severe problems with the attempt to fit the FP23 data to any of the regular structural models: (1) No good fit is found with a sufficiently low RMSD. (2) For all models the best fit corresponds to an order parameter of $S_{\mathrm{mol}} = 1$, leaving no room for variation in this regard. (3) The lowest RMSD values correspond to an α-helix or 3_{10}-helix with a tilt angle of about 90°, which would imply that the peptide lies almost parallel to the membrane surface. However, FP23 does not form an amphipathic helix and is not likely to bind to the membrane surface, because the hydrophobic sequence should be more immersed in the hydrophobic part of the bilayer, which is not supported by this analysis. We therefore have to conclude that this type of RMSD analysis, which is based on regular conformational models, fails for FP23, even though it has been shown to work well for many other membrane-bound peptides.

MD simulations

To generate a structural model of FP23 without having to assume any underlying regular secondary structure, we performed a MD simulation under the influence of the orientational constraints from the ^{19}F-NMR data (MDOC). For this combined data analysis we used a novel approach based on the COSMOS-NMR force field (Sternberg et al. 2006), in which the experimental NMR parameters act as pseudo-forces on the molecular structure (Sternberg et al. 2007). The MDOC program was recently demonstrated to produce reliable orientations and motions of small molecules and larger peptides in membranes (Sternberg et al. 2007). Besides yielding the conformation of a peptide and its alignment in the lipid bilayer, this approach also allows to describe the dynamic flexibility of a molecule over a nanosecond timescale. The all-atom MDOC simulation can be performed with unique speed, as the lipid environment need not be taken into account at a molecular level, but instead acts indirectly as an orienting medium in the form of the orientational constraints *in vacuo* (Sternberg et al. 2007).

After an initial 1 ns MDOC simulation, a second 10 ns MDOC run was performed, taking the final structure and velocities of the first run as a starting point. In the first simulation many conformational changes had been observed, hence we wanted to test the resulting structure for its long-term conformational stability. From the time development of the CF_3 dipolar couplings within the first nanosecond (Fig. 3) it can be seen that the calculated mean values did not smoothly approach their final results, but frequent jumps were indications for conformational changes. These were accompanied by reorientation of the peptide, as depicted in Fig. 4, which illustrates some stages of its structural changes and reorientations. During the first nanosecond the peptide backbone was essentially refolded completely by the orientational constraints. Since the structure of the peptide did not fluctuate about a stable equilibrium, we started another MDOC simulation, using the structure and temperature reached within the previous nanosecond. In this second MD simulation the structure remained nearly unchanged throughout the entire run of 10 ns. When looking at the backbone atoms of the peptide, the RMS deviation of their position was only 1.2 Å, but only 0.26 Å in the last 9 ns. This means that small changes still occurred within the first nanosecond of the long MDOC run, and then the backbone stayed stable for the rest of the time. That also holds for the calculated mean dipolar splittings, changing only within a 1 kHz range.

Since FP23 has an irregular and flexible structure throughout the MDOC simulations, it is best to describe the

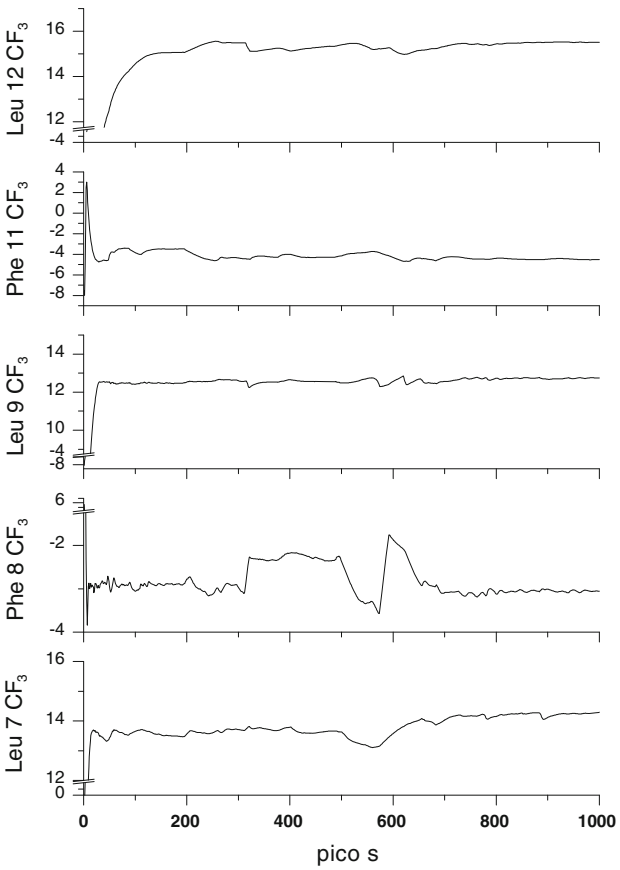

Fig. 3 Time development of the CF_3 dipolar couplings (values in kHz) during a 1 ns MD simulation of FP23. In the second, 10 ns MD simulation only minor changes of the dipolar splittings were observed

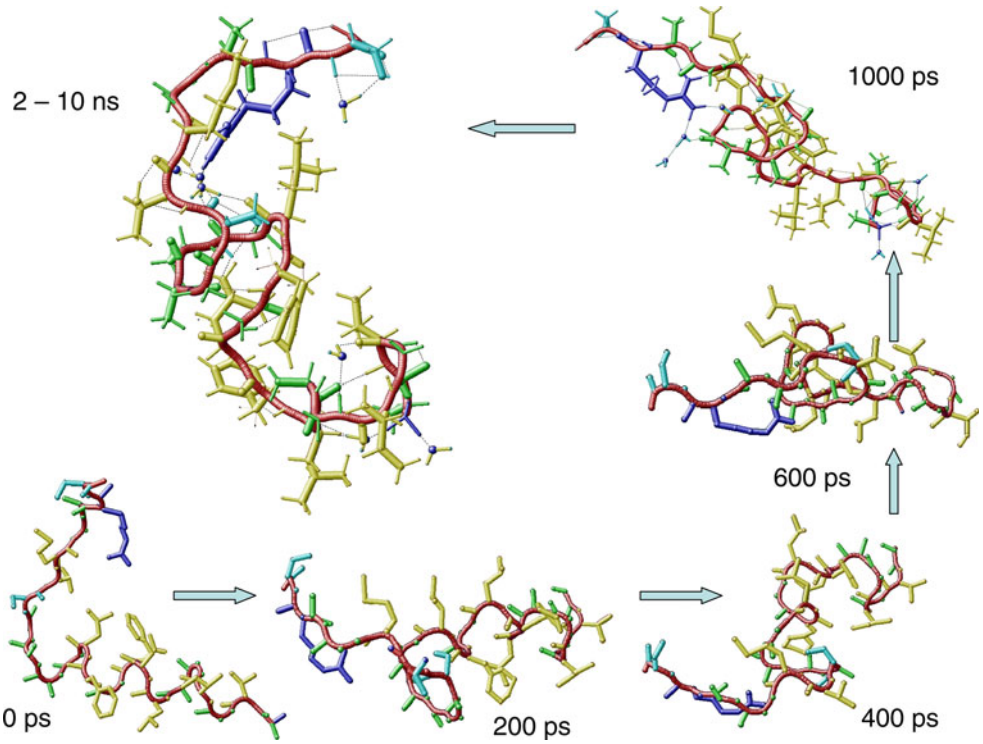

Fig. 4 Structural changes of FP23 in a MD simulation with orientational constraints depicted for two consecutive MD simulations of 1 ns and 10 ns, respectively. The orientation of the membrane normal is upward for all conformers

molecular alignment in terms of its overall tensor of inertia, which can be calculated for every step of the trajectory. In Fig. 5 the time development of this tensor of inertia is depicted during the 10 ns MDOC run. The box illustrates the orientation of the membrane (with the magnetic field pointing upward), and on the unit sphere the fluctuations of the peptide are depicted in terms of its axes of inertia. The axis of least inertia *a* (the long axis of the molecule, depicted in red) changed its orientation within the first nanosecond to a direction where the peptide as a whole is oriented almost upright in the membrane. Its long axis is only tilted by about 16° from the membrane normal (ring of red dots at the top of the unit sphere in Fig. 5). The axis of intermediate inertia (green) jumped for 2 ns to about 80° but stayed most of the time at a tilt of 102°. As can be seen from Fig. 5 the tilt angles are distributed within a range of about 20° around their mean values.

Looking at the resulting structures that are illustrated in Fig. 4 for several stages of the two simulations, it can be clearly seen that the mostly helical starting structure of FP23 is transformed step by step into a bundle of short β-strand-like substructures. This transformation was driven by the orientational pseudo-forces derived from the pseudo-energies which dropped at the end of the simulation to 1,285 kJ/mol. The final mean temperature was only 8 K above the target temperature of 290 K (see ESM). Detailed insight into the conformation can be gained by looking at the time development of the backbone angles φ and ψ for the 10 ns MD as summarized in Fig. 6. The points represent torsion angles sampled every two picoseconds, and the amino acids are indicated by their names and site numbers. At the start of the MD simulation all amino acids lay close together in the region of right-handed α-helices, but the final structure is irregular with a considerable amount of local β-conformations.

Throughout the long MD run, the CF_3 dipolar couplings of each labeled position were calculated and monitored with an exponentially weighted memory time, to obtain mean values representing the final stages of the simulation. As can be seen from Table 1, these time averages are very close to the experimental data, which had been used as input to constrain the MD run. The largest deviation is 3.3 kHz (for a dipolar coupling that can take values between about 16 and −8 kHz), but it should be taken into account that the experimental splittings were measured on five different ^{19}F-labeled peptide analogues whose precise structures may differ slightly. We are therefore confident that the final structure of FP23 obtained after the MD simulation fulfills the NMR constraints and represents a stable energy minimum. It cannot be excluded that other minima with other structures exist, but this question can only be answered when more NMR constraints on the rest of the molecule have been collected (as attempted above by ^{2}H-NMR). A general challenge with this kind of simulation is that there can be a large number of other possible structures that fulfill the

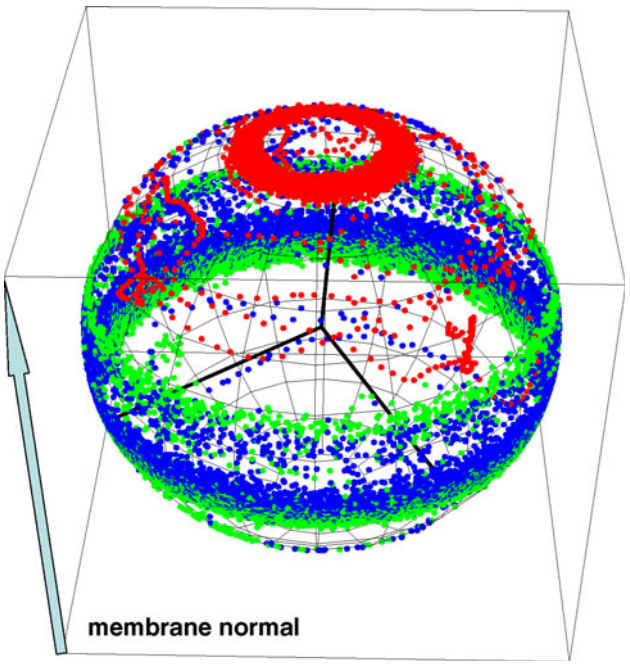

Fig. 5 Cumulative representation of the time development of the principal axes of inertia of FP23 peptide during the 10 ns MDOC simulation. The *box* defines the orientation of the membrane in the horizontal plane, and the magnetic field direction points upward. The bilayer normal thus runs from one pole of the scatter sphere to the other. For the FP23 molecule, in every picosecond time step the instantaneous axes of inertia are calculated and displayed on the sphere. The axis of least inertia *a* is shown in *red*, the axis of highest inertia is shown in *blue*, and that of intermediate inertia in *green*, and their final orientations are indicated by *black lines*. Overall, the long axis *a* of the peptide maintains an alignment nearly parallel to the membrane normal

constraints as well. With regard to the dipolar couplings, the orientation of every C–CF_3 bond vector relative to the membrane normal is twofold degenerate, leading to two possible orientations of every labeled group. To find all possible peptide structures or even to examine statistically the most populated conformational state, we would have to generate a large set of molecules and select the most favored conformers from their energies and pseudo-energies. Therefore, at this point we can only state that the structure described here (Figs. 4, 7) is a feasible model, whose conformation and molecular alignment in the membrane are consistent with the NMR data, and which is energetically stable over a long MD period.

Analysis of the MD trajectory has also yielded the local order parameters S^i_{loc} for each of the ^{19}F-labeled segments. A strong variation is observed along the labeled stretch of the peptide sequence. The loop in the center of the molecule is stabilized by hydrogen bonds from Ser17 to the backbone and by another one from the Phe11 amide to the Ala15 carbonyl, leaving Phe8 very mobile. The overall molecular order parameter S_{mol} is 0.82 with a biaxiality of 0.01, and these values are in a normal range for peptides. We note here a situation where the order in some segments may be much lower than the order of the molecule as a whole. The observed irregular structure together with the strong variation of S^i_{loc} explains why a simple analysis of the peptide orientation using a regular secondary structure has not been possible. Concerning the insertion of FP23 into the membrane, a likely scenario is illustrated in Fig. 7. With the charged Arg22 located near the lipid head group region, the more hydrophobic stretch of the molecule is nicely seen to be embedded in the bilayer core. Even though we did not measure explicit constraints for the first few amino acids, it is seen that a stable conformation is formed when the N-terminal amino group folds back in a loop that is stabilized by hydrogen bonds.

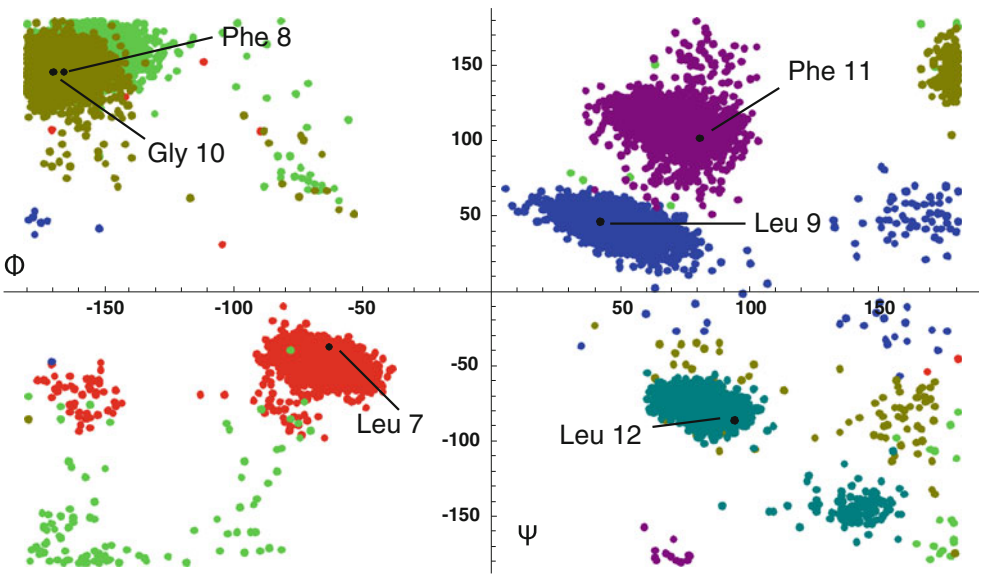

Fig. 6 Cumulative representation of the time development of the backbone angles φ and ψ during the 10 ns MDOC simulation of FP23, shown as a Ramachandran plot sampled every two picoseconds. The central stretch of amino acids in the peptide is displayed that was under the influence of the orientational constraints (Leu7 in *red*, Phe8 in *green*, Leu9 in *blue*, Gly10 in *olive*, Phe11 in *magenta*, and Leu12 in *dark green*). The *black dots* indicate the angular pairs seen at the end of the MDOC simulation

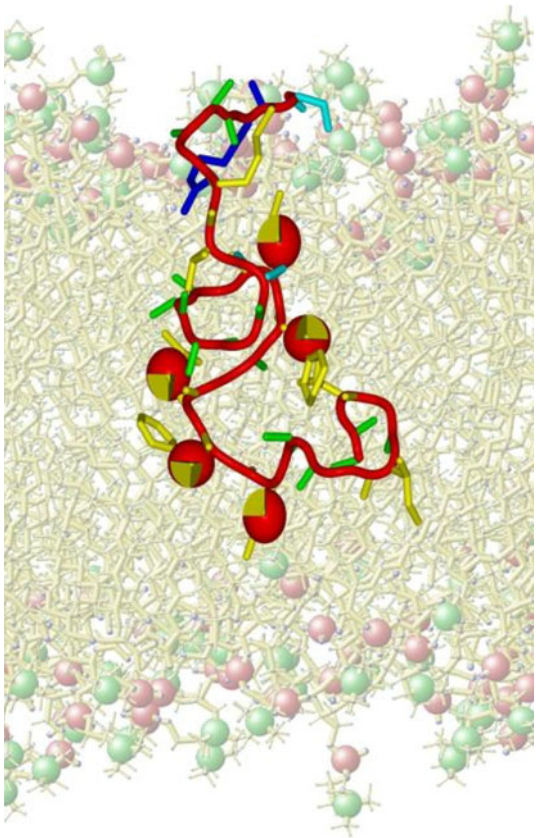

Fig. 7 Putative conformation and insertion of FP23 in the membrane, illustrating the irregular structure and the upright orientation of the peptide long-axis. (The lipid molecules did not enter the simulation.) Each selective ^{19}F-label is displayed with its dipolar tensor ellipsoid of the CF_3-group, which provided the orientational constraints for the MDOC simulation. The cut sphere segments indicate the orientation of the principal axes of the tensors

Conclusions

Solid-state ^{19}F-NMR analysis of selectively CF_3-labeled peptides can yield a wealth of information about their molecular structures and dynamic behavior. However, in the present case of the HIV fusion peptide FP23, no consistent picture could be obtained using the established approach of data analysis, which has to rely on a regular backbone structure and uniform local order along the peptide chain. Nonetheless, several meaningful conclusions can be drawn from our ^{19}F-, ^{2}H-, and ^{31}P-NMR observations of five selective CF_3-Phg labels and four selective D_3-Ala labels in the peptide embedded in phospholipid model membranes: (1) All FP23 molecules in the ensemble assume one and the same structure (as a time average over milliseconds) in liquid-crystalline DMPC bilayers at a peptide-to-lipid ratio of 1:300 (measured at 35°C and 96% humidity). (2) This homogeneous structure is neither isotropically averaged nor aggregated, but the individual molecular segments show distinctly different preferred local orientations in the membrane. (3) The peptide conformation is not compatible with any regular secondary structure, such as an α-helix, 3_{10}-helix, π-helix or β-strand (neither planar nor twisted). (4) The peptides undergo unrestricted lateral diffusion and rotation in the bilayer plane on a millisecond timescale, which implies the presence of monomers or small oligomers. (5) Some dynamic processes also seem to occur on a microsecond timescale (interfering with ^{2}H-NMR echo experiments). (6) FP23 becomes immobilized and loses its preferred alignment in the membrane at a higher peptide concentration (P/L = 1:30 in DMPC), which confirms a tendency for aggregation that is favored by the presence of negatively charged lipids such as POPC/POPG. (7) In the presence of excess water, FP23 has only a moderate affinity for DMPC and partitions into the aqueous phase in a slow, two-state equilibrium on a millisecond timescale. (8) The lipid bilayer remains quite unperturbed by the presence of FP23, even when it aggregates.

As structure determination of FP23 in DMPC was not possible from the NMR data alone, all-atom MD simulations were carried out with the orientational NMR constraints and produced a stable though irregular structure, stabilized by intramolecular hydrogen bonds. The peptide forms some loop-like turns and has a high content of local β-conformations, in accordance with previous ^{13}C carbonyl chemical shift measurements of membrane-bound FP23 (Sackett and Shai 2003). Our MD results suggest considerable differences in the local segmental mobilities along the peptide sequence, as expected for such irregular backbone structure. We found that the long axis of the peptide, as defined by its axis of least inertia, is aligned almost parallel to the membrane normal, which is consistent with an inserted state of the hydrophobic N-terminus. Other studies of FP23 have suggested α-helical structures with sometimes very steep insertion angles, or β-structures (Maddox and Longo 2002; Peuvot et al. 1999; Yang and Weliky 2003; Yang et al. 2003). However, it remains questionable whether these methods could have picked up or properly interpreted the irregular FP23 structure that is seen in the present study. Our results are based on ^{19}F-NMR labels positioned along the central stretch of amino acids 6–15, and there are still some ambiguities in the uniqueness of the proposed model, especially with regard to the terminal regions at either end. Further studies will thus be needed to clarify whether the remaining parts of FP23 really show such intriguing conformation as suggested here. Nevertheless, our study has revealed some fundamental properties of FP23 in lipid membranes, which may not have been expected based on previous, more qualitative structural reports. These results on FP23 might even represent a group of "intrinsically unstructured" peptides and

proteins that are still highly flexible when attached to the two-dimensional plane of a lipid membrane.

Acknowledgments We thank Johannes Reichert and Jochen Bürck for their help with the lipid mixing assays, dynamic light scattering measurements, and CD spectroscopy, Sergii Afonin and Olaf Zwernemann for their advice on peptide synthesis and purification, Igor Jakovkin for performing the statistical analysis on the peptide backbone, and Carl Philipp Ulrich for his constructive comments. The project was partially funded by the DFG-Center for Functional Nanostructures (E1.2).

References

Afonin S, Glaser RW, Berditchevskaia M, Wadhwani P, Guhrs KH, Mollmann U, Perner A, Ulrich AS (2003) 4-Fluorophenylglycine as a label for ^{19}F-NMR structure analysis of membrane-associated peptides. Chembiochem 4:1151–1163

Afonin S, Dürr UHN, Glaser RW, Ulrich AS (2004) 'Boomerang'-like insertion of a fusogenic peptide in a lipid membrane revealed by solid-state ^{19}F NMR. Magn Reson Chem 42:195–203

Afonin S, Dürr UHN, Wadhwani P, Salgado JB, Ulrich AS (2008a) Solid state NMR structure analysis of the antimicrobial peptide gramicidin S in lipid membranes: concentration-dependent re-alignment and self-assembly as a β-barrel. Topics Curr Chem 273:139–154

Afonin S, Grage SL, Ieronimo M, Wadhwani P, Ulrich AS (2008b) Temperature-dependent transmembrane insertion of the amphiphilic peptide PGLa in lipid bilayers observed by solid state ^{19}F-NMR spectroscopy. J Am Chem Soc 130:16512–16514

Allen FH, Kennard O, Watson DG, Brammer L, Orpen AG, Taylor R (1987) Tables of bond lengths determined by X-ray and neutron diffraction.1. Bond lengths in organic compounds. J Chem Soc Perkin Trans 2:S1–S19

Barz B, Wong TC, Kosztin I (2008) Membrane curvature and surface area per lipid affect the conformation and oligomeric state of HIV-1 fusion peptide: a combined FTIR and MD simulation study. Biochim Biophys Acta 1778:945–953

Bodner ML, Gabrys CM, Struppe JO, Weliky DP (2008) 13C–13C and 15 N–13C correlation spectroscopy of membrane-associated and uniformly labeled human immunodeficiency virus and influenza fusion peptides: amino acid-type assignments and evidence for multiple conformations. J Chem Phys 128:052319

Buchschacher GL Jr, Freed EO, Panganiban AT (1995) Effects of second-site mutations on dominant interference by a human immunodeficiency virus type 1 envelope glycoprotein mutant. J Virol 69:1344–1348

Castano S, Desbat B (2005) Structure and orientation study of fusion peptide FP23 of gp41 from HIV-1 alone or inserted into various lipid membrane models (mono-, bi- and multibi-layers) by FT-IR spectroscopies and Brewster angle microscopy. Biochim Biophys Acta 1715:81–95

Chang DK, Cheng SF, Chien WJ (1997a) The amino-terminal fusion domain peptide of human immunodeficiency virus type 1 gp41 inserts into the sodium dodecyl sulfate micelle primarily as a helix with a conserved glycine at the micelle-water interface. J Virol 71:6593–6602

Chang DK, Chien WJ, Cheng SF (1997b) The FLG motif in the N-terminal region of glucoprotein 41 of human immunodeficiency virus type 1 adopts a type-I beta turn in aqueous solution and serves as the initiation site for helix formation. Eur J Biochem 247:896–905

Chang DK, Cheng SF, Trivedi VD (1999) Biophysical characterization of the structure of the amino-terminal region of gp41 of HIV-1. Implications on viral fusion mechanism. J Biol Chem 274:5299–5309

Delahunty MD, Rhee I, Freed EO, Bonifacino JS (1996) Mutational analysis of the fusion peptide of the human immunodeficiency virus type 1: identification of critical glycine residues. Virology 218:94–102

Durell SR, Martin I, Ruysschaert JM, Shai Y, Blumenthal R (1997) What studies of fusion peptides tell us about viral envelope glycoprotein-mediated membrane fusion. Mol Membr Biol 14:97–112

Dürr UHN (2005) ^{19}F-NMR studies on fluorine-labeled model compounds and biomolecules Biochemistry. Ph D thesis, University of Karlsruhe, Karlsruhe

Esteban-Martín S, Strandberg E, Fuertes G, Ulrich AS, Salgado J (2009) Influence of whole-body dynamics on ^{15}N PISEMA NMR spectra of membrane peptides: a theoretical analysis. Biophys J 96:3233–3241

Esteban-Martín S, Strandberg E, Salgado J, Ulrich AS (2010) Solid state NMR analysis of peptides in membranes: influence of dynamics and labeling scheme. Biochim Biophys Acta 1798:252–257

Evans J, Morris GP (1990) Statistical mechanics of nonequilibrium liquids. Academic Press, London

Gabrys CM, Weliky DP (2007) Chemical shift assignment and structural plasticity of a HIV fusion peptide derivative in dodecylphosphocholine micelles. Biochim Biophys Acta 1768:3225–3234

Gerber D, Pritsker M, Gunther-Ausborn S, Johnson B, Blumenthal R, Shai Y (2004) Inhibition of HIV-1 envelope glycoprotein-mediated cell fusion by a DL-amino acid-containing fusion peptide: possible recognition of the fusion complex. J Biol Chem 279:48224–48230

Glaser RW, Grüne M, Wandelt C, Ulrich AS (1999) NMR and CD structural analysis of the fusogenic peptide sequence B18 from the fertilization protein bindin. Biochemistry 38:2560–2569

Glaser RW, Sachse C, Dürr UHN, Wadhwani P, Ulrich AS (2004) Orientation of the antimicrobial peptide PGLa in lipid membranes determined from ^{19}F-NMR dipolar couplings of 4-CF_3-phenylglycine labels. J Magn Reson 168:153–163

Glaser RW, Sachse C, Dürr UHN, Afonin S, Wadhwani P, Strandberg E, Ulrich AS (2005) Concentration-dependent realignment of the antimicrobial peptide PGLa in lipid membranes observed by solid-state ^{19}F-NMR. Biophys J 88:3392–3397

Gordon LM, Mobley PW, Pilpa R, Sherman MA, Waring AJ (2002) Conformational mapping of the N-terminal peptide of HIV-1 gp41 in membrane environments using ^{13}C-enhanced Fourier transform infrared spectroscopy. Biochim Biophys Acta 1559:96–120

Gordon LM, Mobley PW, Lee W, Eskandari S, Kaznessis YN, Sherman MA, Waring AJ (2004) Conformational mapping of the N-terminal peptide of HIV-1 gp41 in lipid detergent and aqueous environments using ^{13}C-enhanced Fourier transform infrared spectroscopy. Protein Sci 13:1012–1030

Gordon LM, Nisthal A, Lee AB, Eskandari S, Ruchala P, Jung CL, Waring AJ, Mobley PW (2008) Structural and functional properties of peptides based on the N-terminus of HIV-1 gp41 and the C-terminus of the amyloid-beta protein. Biochim Biophys Acta 1778:2127–2137

Grage SL, Afonin S, Ulrich AS (2010) Dynamic transitions of membrane active peptides. Meth Mol Biol 618:183–207

Haque ME, Koppaka V, Axelsen PH, Lentz BR (2005) Properties and structures of the influenza and HIV fusion peptides on lipid membranes: implications for a role in fusion. Biophys J 89:3183–3194

Jaroniec CP, Kaufman JD, Stahl SJ, Viard M, Blumenthal R, Wingfield PT, Bax A (2005) Structure and dynamics of micelle-associated human immunodeficiency virus gp41 fusion domain. Biochemistry 44:16167–16180

Kanyalkar M, Srivastava S, Saran A, Coutinho E (2004) Conformational study of fragments of envelope proteins (gp120: 254–274 and gp41: 519–541) of HIV-1 by NMR and MD simulations. J Pept Sci 10:363–380

Kliger Y, Aharoni A, Rapaport D, Jones P, Blumenthal R, Shai Y (1997) Fusion peptides derived from the HIV type 1 glycoprotein 41 associate within phospholipid membranes and inhibit cell-cell fusion. Structure-function study. J Biol Chem 272:13496–13505

Li Y, Tamm LK (2007) Structure and plasticity of the human immunodeficiency virus gp41 fusion domain in lipid micelles and bilayers. Biophys J 93:876–885

Maddox MW, Longo ML (2002) Conformational partitioning of the fusion peptide of HIV-1 gp41 and its structural analogs in bilayer membranes. Biophys J 83:3088–3096

Maisch D, Wadhwani P, Afonin S, Koksch B, Ulrich AS (2009) Chemical labeling strategy with (R)- and (S)-triofluoromethylalanin for solid state ^{19}F-NMR analysis of peptaibols in membranes. J Am Chem Soc 131:15596–15597

Marsan MP, Muller I, Ramos C, Rodriguez F, Dufourc EJ, Czaplicki J, Milon A (1999) Cholesterol orientation and dynamics in dimyristoylphosphatidylcholine bilayers: a solid state deuterium NMR analysis. Biophys J 76:351–359

Mobley PW, Waring AJ, Sherman MA, Gordon LM (1999) Membrane interactions of the synthetic N-terminal peptide of HIV-1 gp41 and its structural analogs. Biochim Biophys Acta 1418:1–18

Mykhailiuk PK, Afonin S, Chernega AN, Rusanov EB, Platonov MO, Dubinina GG, Berditsch M, UIrich AS, Komarov IV (2006) Conformationally rigid trifluoromethyl-substituted α-amino acid designed for peptide structure analysis by solid-state ^{19}F NMR spectroscopy. Angew Chem Int Ed Engl 45:5659–5661

Mykhailiuk PK, Afonin S, Palamarchuk GV, Shishkin OV, Ulrich AS, Komarov IV (2008) Synthesis of trifluoromethyl-substituted proline analogues as ^{19}F NMR labels for peptides in the polyproline II conformation. Angew Chem Int Ed Engl 47:5765–5767

Peisajovich SG, Epand RF, Pritsker M, Shai Y, Epand RM (2000) The polar region consecutive to the HIV fusion peptide participates in membrane fusion. Biochemistry 39:1826–1833

Pereira FB, Goni FM, Muga A, Nieva JL (1997) Permeabilization and fusion of uncharged lipid vesicles induced by the HIV-1 fusion peptide adopting an extended conformation: dose and sequence effects. Biophys J 73:1977–1986

Peuvot J, Schanck A, Lins L, Brasseur R (1999) Are the fusion processes involved in birth, life and death of the cell depending on tilted insertion of peptides into membranes? J Theor Biol 198:173–181

Pritsker M, Jones P, Blumenthal R, Shai Y (1998) A synthetic all D-amino acid peptide corresponding to the N-terminal sequence of HIV-1 gp41 recognizes the wild-type fusion peptide in the membrane and inhibits HIV-1 envelope glycoprotein-mediated cell fusion. Proc Natl Acad Sci U S A 95:7287–7292

Pritsker M, Rucker J, Hoffman TL, Doms RW, Shai Y (1999) Effect of nonpolar substitutions of the conserved Phe11 in the fusion peptide of HIV-1 gp41 on its function, structure, and organization in membranes. Biochemistry 38:11359–11371

Qiang W, Weliky DP (2009) HIV fusion peptide and its cross-linked oligomers: efficient syntheses, significance of the trimer in fusion activity, correlation of beta strand conformation with membrane cholesterol, and proximity to lipid headgroups. Biochemistry 48:289–301

Qiang W, Yang J, Weliky DP (2007) Solid-state nuclear magnetic resonance measurements of HIV fusion peptide to lipid distances reveal the intimate contact of beta strand peptide with membranes and the proximity of the Ala-14-Gly-16 region with lipid headgroups. Biochemistry 46:4997–5008

Qiang W, Bodner ML, Weliky DP (2008) Solid-state NMR spectroscopy of human immunodeficiency virus fusion peptides associated with host-cell-like membranes: 2D correlation spectra and distance measurements support a fully extended conformation and models for specific antiparallel strand registries. J Am Chem Soc 130:5459–5471

Qiang W, Sun Y, Weliky DP (2009) A strong correlation between fusogenicity and membrane insertion depth of the HIV fusion peptide. Proc Natl Acad Sci U S A 106:15314–15319

Rafalski M, Lear JD, DeGrado WF (1990) Phospholipid interactions of synthetic peptides representing the N-terminus of HIV gp41. Biochemistry 29:7917–7922

Reichert J, Grasnick D, Afonin S, Buerck J, Wadhwani P, Ulrich AS (2007) A critical evaluation of the conformational requirements of fusogenic peptides in membranes. Eur Biophys J 36:405–413

Sackett K, Shai Y (2002) The HIV-1 gp41 N-terminal heptad repeat plays an essential role in membrane fusion. Biochemistry 41:4678–4685

Sackett K, Shai Y (2003) How structure correlates to function for membrane associated HIV-1 gp41 constructs corresponding to the N-terminal half of the ectodomain. J Mol Biol 333:47–58

Sackett K, Nethercott M, Shai Y, Weliky D (2009) Hairpin folding of HIV gp41 abrogates lipid mixing function at physiologic pH and inhibits lipid mixing by exposed gp41 constructs. Biochemistry 48:2714–2722

Sackett K, Nethercott MJ, Epand RF, Epand RM, Kindra DR, Shai Y, Weliky DP (2010) Comparative analysis of membrane-associated fusion peptide secondary structure and lipid mixing function of HIV gp41 constructs that model the early pre-hairpin intermediate and final hairpin conformations. J Mol Biol 397:301–315

Salgado J, Grage SL, Kondejewski LH, Hodges RS, McElhaney RN, Ulrich AS (2001) Membrane-bound structure and alignment of the antimicrobial β-sheet peptide gramicidin S derived from angular and distance constraints by solid state ^{19}F-NMR. J Biomol NMR 21:191–208

Sternberg U, Koch F-T, Losso P (2006) COSMOS program. COSMOS Software, Jena

Sternberg U, Witter R, Ulrich AS (2007) All-atom molecular dynamics simulations using orientational constraints from anisotropic NMR samples. J Biomol NMR 38:23–39

Strandberg E, Ulrich AS (2004) NMR methods for studying membrane-active antimicrobial peptides. Concepts Magn Reson A 23A:89–120

Strandberg E, Özdirekcan S, Rijkers DTS, Van der Wel PCA, Koeppe RE, II, Liskamp RMJ, Killian JA (2004) Tilt angles of transmembrane model peptides in oriented and non-oriented lipid bilayers as determined by ^{2}H solid state NMR. Biophys J 86:3709–3721

Strandberg E, Wadhwani P, Tremouilhac P, Dürr UHN, Ulrich AS (2006) Solid-state NMR analysis of the PGLa peptide orientation in DMPC bilayers: structural fidelity of ^{2}H-labels versus high sensitivity of ^{19}F-NMR. Biophys J 90:1676–1686

Strandberg E, Kanithasen N, Tiltak D, Bürck J, Wadhwani P, Zwernemann O, Ulrich AS (2008) Solid-state NMR analysis comparing the designer-made antibiotic MSI-103 with its parent peptide PGLa in lipid bilayers. Biochemistry 47:2601–2616

Strandberg E, Esteban-Martín S, Salgado J, Ulrich AS (2009) Orientation and dynamics of peptides in membranes calculated from ^{2}H-NMR data. Biophys J 96:3223–3232

Tremouilhac P, Strandberg E, Wadhwani P, Ulrich AS (2006a) Conditions affecting the re-alignment of the antimicrobial peptide PGLa in membranes as monitored by solid state ^{2}H-NMR. Biochim Biophys Acta 1758:1330–1342

Tremouilhac P, Strandberg E, Wadhwani P, Ulrich AS (2006b) Synergistic transmembrane alignment of the antimicrobial heterodimer PGLa/magainin. J Biol Chem 281:32089–32094

Ulrich AS (2005) Solid state ^{19}F-NMR methods for studying biomembranes. Progr Nucl Magn Reson Spectrosc 46:1–21

Ulrich AS (2007) Solid state ^{19}F-NMR analysis of oriented biomembranes. In: Webb GA (ed) Modern magnetic resonance, vol 1. Springer, Dordrecht, pp 261–267

Ulrich AS, Tichelaar W, Förster G, Zschörnig O, Weinkauf S, Meyer HW (1999) Ultrastructural characterization of peptide-induced membrane fusion and peptide self-assembly in the bilayer. Biophys J 77:829–841

Ulrich AS, Wadhwani P, Dürr UHN, Afonin S, Glaser RW, Strandberg E, Tremouilhac P, Sachse C, Berditchevskaia M, Grage SL (2006) Solid-state ^{19}F-nuclear magnetic resonance analysis of membrane-active peptides. In: Ramamoorthy A (ed) NMR spectroscopy of biological solids. CRC Press, Boca Raton, pp 215–236

Wadhwani P, Bürck J, Strandberg E, Mink C, Afonin S, Ulrich AS (2008) Using a sterically restrictive amino acid as a ^{19}F-NMR label to monitor and control peptide aggregation in membranes. J Am Chem Soc 130:16515–16517

Wadhwani P, Reichert J, Bürck J, Ulrich AS (2010) Antimicrobial and cell penetrating peptides can trigger membrane fusion by folding and aggregation (submitted)

Wasniewski CM, Parkanzky PD, Bodner ML, Weliky DP (2004) Solid-state nuclear magnetic resonance studies of HIV and influenza fusion peptide orientations in membrane bilayers using stacked glass plate samples. Chem Phys Lipids 132:89–100

White JM, Delos SE, Brecher M, Schornberg K (2008) Structures and mechanisms of viral membrane fusion proteins: multiple variations on a common theme. Crit Rev Biochem Mol Biol 43:189–219

Wong TC (2003) Membrane structure of the human immunodeficiency virus gp41 fusion peptide by molecular dynamics simulation. II. The glycine mutants. Biochim Biophys Acta 1609:45–54

Yang J, Weliky DP (2003) Solid-state nuclear magnetic resonance evidence for parallel and antiparallel strand arrangements in the membrane-associated HIV-1 fusion peptide. Biochemistry 42:11879–11890

Yang J, Gabrys CM, Weliky DP (2001) Solid-state nuclear magnetic resonance evidence for an extended β strand conformation of the membrane-bound HIV-1 fusion peptide. Biochemistry 40: 8126–8137

Yang R, Yang J, Weliky DP (2003) Synthesis, enhanced fusogenicity, and solid state NMR measurements of cross-linked HIV-1 fusion peptides. Biochemistry 42:3527–3535

Yang R, Prorok M, Castellino FJ, Weliky DP (2004) A trimeric HIV-1 fusion peptide construct which does not self-associate in aqueous solution and which has 15-fold higher membrane fusion rate. J Am Chem Soc 126:14722–14723

Zheng Z, Yang R, Bodner ML, Weliky DP (2006) Conformational flexibility and strand arrangements of the membrane-associated HIV fusion peptide trimer probed by solid-state NMR spectroscopy. Biochemistry 45:12960–12975